Mass Change Hybrid SST-QGG Technology Report

POC: Nan Yu (nan.yu@jpl.nasa.gov)
Prepared with Sheng-wey Chiow (sheng-wey.chiow@jpl.nasa.gov) and
Srinivas Bettadpur (srinivas@csr.utexas.edu)

Technology Description

The basis of the quantum gravity gradiometer (QGG)[1] is the use of laser cooled ultra-cold atoms as ideal test masses and the quantum matter-wave property for atom-interferometer (AI) displacement measurements. Using an approach similar to high precision atomic clocks, atomic sensors are capable of highly sensitive and stable measurements with the flat noise power spectrum to very low frequencies. For instance, atomic accelerometers allow access to below μHz and close to 1 Hz with equally low noise power while electrostatic accelerometers have rapid noise increase below 5 mHz [2].

Taking advantage of these capabilities, atomic gradiometers have been proposed to significantly improve future earth time-varying gravity measurements. Gradiometers can be used in a single spacecraft as in the GOCE mission [2-9]. More recently, we showed that simple single-axis gradiometers can also be used in the usual satellite-to-satellite tracking (SST) configuration with great science measurement enhancements. Such a hybrid architecture provides immediate science benefit by mitigating the principal aliasing error limitation of mass change measurement using SST alone [10-12], while offering a low-risk technology infusion path for future gradiometer-based missions.

Technology SOA

Current laboratory-based as well as transportable QGG have demonstrated sensitivities at the level of 10's $E/\sqrt{Hz}$ using 10^6 cold thermal atoms (microkelvin, μK) with 1-Hz data rate and about 1-m baselines [13]. These early versions of gradiometers are relatively mature. For example, JPL developed a Transportable Quantum Gravity Gradiometer under ESTO-IIP nearly 10 years ago. A sensitivity of 40 $E/\sqrt{Hz}$ was demonstrated both by in-loop residual error and by external proximity modulation of 30 kg lead bricks [13]. The QGG was specifically designed to be compatible with microgravity environments, so that the instrument would operate as is in free flight. It was thus assessed to reach TRL 5 in 2015.

Recently, GSFC, working with AOsense, is in the process of demonstrating another version of the gradiometer with high-flux colder atom sources [4-9] and aims at achieving $mE/\sqrt{Hz}$ level of sensitivity with 1-Hz data rate and 1-m baseline. Extrapolating to the extended interrogation time available in microgravity in space leads to the estimation of 50 $\mu E/\sqrt{Hz}$ sensitivity with reduced data rate of 0.03 Hz [9]. More recently, a European company has demonstrated a commercial terrestrial gradiometer with sensitivity close to the ground based SOA [14].

At the same time, JPL, working with NASA Biological and Physical Science Division, has developed and operated the Cold Atom Laboratory (CAL) onboard ISS since 2018, in which ultra-cold atoms of pK have been produced daily and atom interferometer in space investigations are one of the main objectives [15, 16]. CAL is a technology pathfinder for AI in

space, though the multi-purpose facility has limited ability to perform precision measurements required by Earth gravity measurements.

In our assessment, sensitivity below 0.5 $mE/\sqrt{Hz}$ can be achieved with the already demonstrated methods in realizing atom interferometers. However, a much greater sensitivity of 10 $\mu E/\sqrt{Hz}$ can be achieved with a number of new methods in implementing atom interferometers including use of quantum squeezed states for below quantum projection noise detections (see below) that could be validated and matured in the next few years.

Technology Maturation and Infusion

The Center for Space Research (CSR) at UT Austin and JPL have collaborated in developing a hybrid architecture for effective infusion of quantum gravity gradiometer (QGG) instruments together with conventional satellite-to-satellite tracking (SST) for spaceborne mass change measurements. This hybrid architecture leverages the success of both the GRACE satellite-to-satellite tracking (SST) configuration and the unprecedented performance of QGG for Earth science gravity measurements in LEO. The configuration consists of GRACE-like SST between two spacecraft, and a single-axis atomic gravity gradiometer onboard each of the twin satellites along the cross-track direction, as depicted in Figure 1. The hybrid configuration is placed in a near polar, ≈ 500 km altitude circular orbit. In contrast, an architecture with only a QGG instrument for mass change must fly at much lower altitudes, with no assurance of a long data record. The cross-track QGG accommodation provides gradient measurements along the spacecraft pitch axis. This orientation can be shown [17] to be least sensitive to errors in the knowledge of the instrument (or spacecraft) orientation and rates of angular motion.

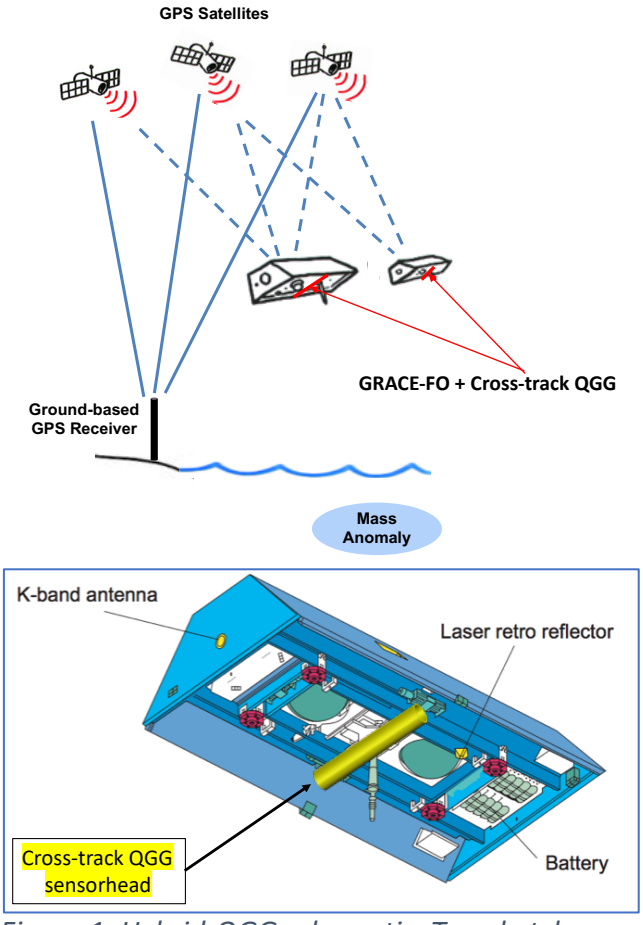

Figure 1. Hybrid-QGG schematic. Top sketch shows the SST-QGG mission architecture, whereas lower graph depicts a possible accommodation of QGG sensor head in a GRACE spacecraft.

Our assessments of this hybrid configuration using numerical simulations clearly shows that gravity gradient information from the QGG can significantly boost the results from the GRACE-like configuration. Figure 2 shows the gravity field precision requirements (upper bounds) allocated solely to the instrument systems in green. The best-case outcomes from numerical simulation

of GRACE Follow-On SST, accelerometer, and pointing specifications are shown in gray. The pair of curves in blue and red show that a mass change measurement configuration using only a 10 $\mu E/\sqrt{Hz}$ QGG oriented in the radial direction must orbit at 250 km altitude before it significantly improves upon the SST or the hybrid configurations. The degradation at the low-degree harmonics when orbiting at 450 km is particularly significant given the importance of these modes of the Earth gravity field for measurement of time-variations. By contrast, the pink curve shows that it is possible to obtain meaningful improvement in science outcomes from an SST mission by hybridizing it with a QGG. Further details of this improvement will be provided in the next section.

Based on the initial findings, with the demonstrated approaches realizing the performance at 10's of $mE/\sqrt{Hz}$, tangible impact and improvement to GRACE-FO can be expected, therefore the aforementioned science requirement threshold. A successful demonstration of the atom interferometric technology in the hybrid configuration offers a rapid technology infusion pathway, thereby paving the way for future quantum gravity gradiometer missions for Earth science as well as other space applications.

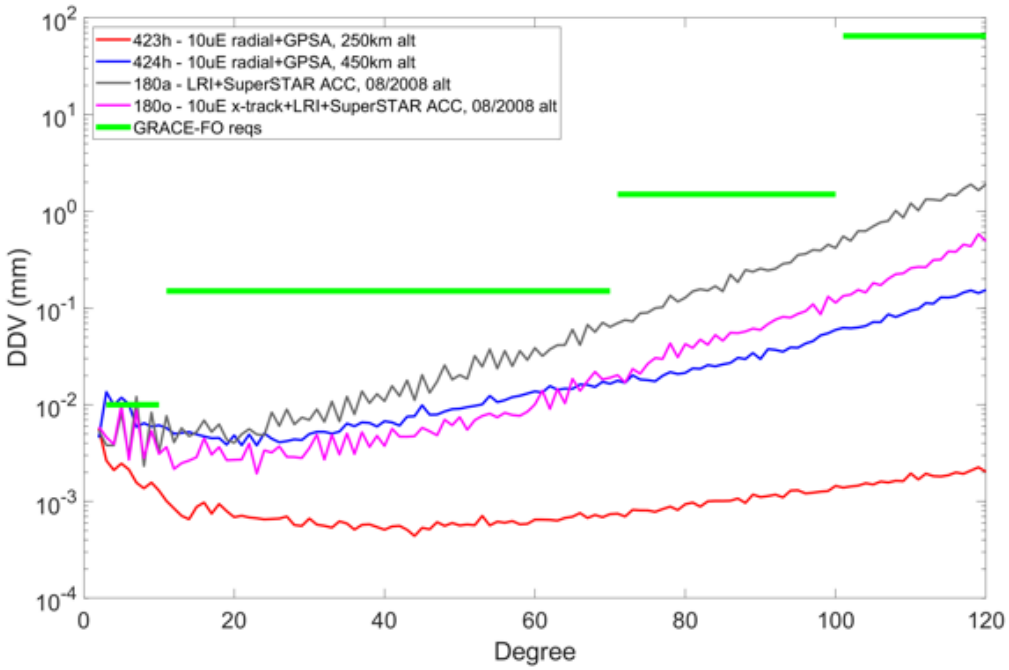

Figure 2. Simulation results of various configurations. Green segments: GRACE requirements. Black: GRACE-FO instrument performance. Blue: single spacecraft radial gravity gradiometer at altitude 450km. Pink: hybrid SST+QGG configuration at altitude ~500km. Red: single spacecraft radial gravity gradiometer at altitude 250km.

Hybrid architecture Time Variable Gravity Performance

Numerous pathways exist to surmount the current measurement system limitations on the use of SST for time-variable mass change measurements – examples include reduction of noise in the metrology; the use of more complex flight configuration that allow lower altitude

orbits for increased signals while permitting longer lifetime; and – of interest here – the infusion of the QGG technology into an SST configuration. However, the greatest challenge facing the SST techniques is “aliasing” or “striping” - the manifestation of systematic errors as specific spatial-temporal patterns that are known to be the limiting error in scientific exploitation of data from GRACE and GRACE-FO. The systematic errors arise from our imperfect knowledge of rapid gravitational variations that cannot be sensed by SST mission global sampling strategy, and must be thereby modeled based on prior or independent knowledge.

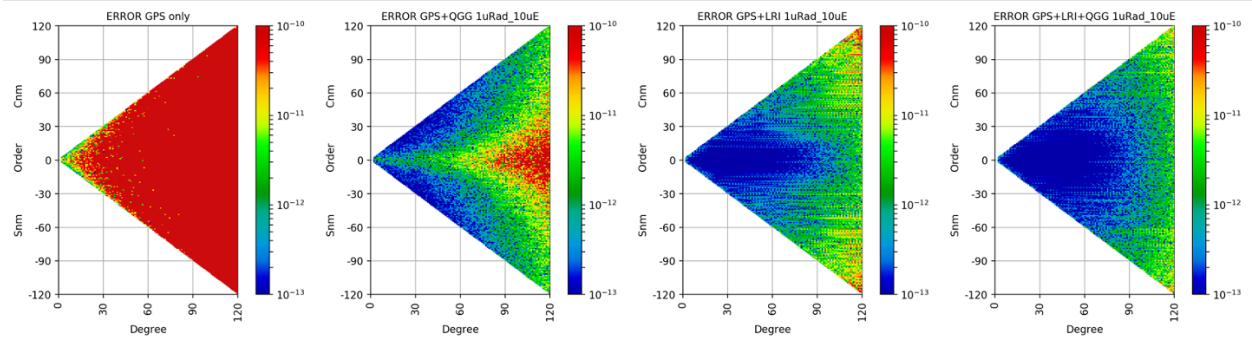

Figure 3 Each figure illustrates the errors in the recovery of the gravity field from each data-type. Low numbers (blue colors) indicate small errors (or greater accuracy). Left panel shows that GPS contributes only the longest wavelength (low-degree) harmonics; QGG contributes to the sectorial (n=m) harmonics; and by contrast, SST contributes to the near-zonals.

Figure 3 shows the QGG and the LRI contribute the best information (middle two panels) to very complementary modes of the gravity field – the former to the near-sectorial harmonics; and the latter to the near zonals. Aliasing errors in the SST constellation can be shown to be predominantly manifested in the near-sectorial harmonics. Hybridization of a QGG with an SST mission therefore offers an effective means of controlling the aliasing error while improving the overall quality of the gravity field.

As an illustration, Figure 4 shows the results from a numerical simulation of a hybrid SST+QGG mission, where the QGG is carried in the cross-track direction. The logic for this particular geometry of hybridization is discussed in the next section. This numerical simulation result clearly shows the dramatic reduction in the typical resonant and sectorial order errors arising from the SST upon the addition of the QGG data-type.

While the benefits of the hybrid QGG configuration remain validated, the amount of possible improvement in the overall gravity field recovery is dependent on several design choices. As the altitude is lowered, the quality of the field improves faster for the QGG dataset when compared to the SST dataset. Improvement in the quality of the QGG metrology from 100 to 1 $\mu E/\sqrt{Hz}$ can have a dramatic impact on the relative quality of the gravity field even at high altitudes. The particular role of the knowledge of the orientation of the QGG is also discussed in the next section.

Overall it is clear that hybridization of QGG with the established SST configuration is an effective means of rapid and significant improvements in mass change measurement, and in particular is a very effective means of mitigating the aliasing error.

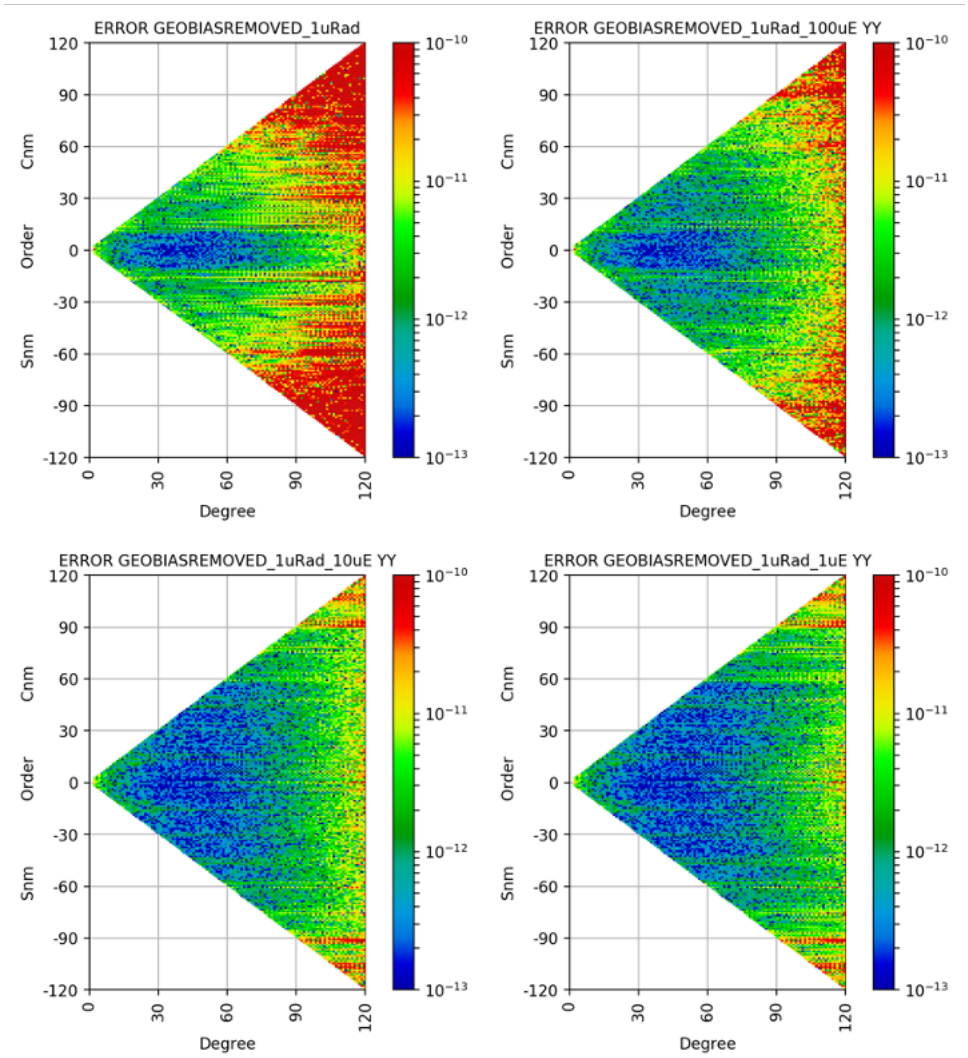

Figure 4. Errors in gravity field recovery in the presence of aliasing errors, showing contributions to error reduction from different data types. The aliasing errors are starkly visible in the top row as increased (yellow-red colors) errors in the resonances (orders near 15 and its multiples) and along the sectorial. These errors are responsible for the characteristic north-south striped error features in geospatial maps. Bottom-row-left panel shows how the reduction in these errors upon the addition of data from the cross-track QGG.

Spacecraft accommodation for QGG in Hybrid architecture

The actual QGG instrument for the hybrid approach is still in the discussion stage, pending on-going science simulation studies and active technology maturation activities. Overall, the dimension of the sensor-head (atomic physics package) is a trade between gradiometer baseline length (and sensitivity) and aerodynamics of spacecraft. Without significantly changing the GRACE-FO spacecraft design for now, the length of the sensor-head would be about 1 meter. A 2-meter sensor-head, which may be possible as the existing spacecraft's base is 2 m, would yield 4x higher sensitivity (detailed on Page. 8), should the science impact warrant the modification of GRACE-FO spacecraft footprint. In addition to the sensor-head, control electronics and laser system are major subsystems (ICE and LOS, to be

detailed on Page. 8). They can be integrated with existing on-board instruments or be distributed to space available within the spacecraft envelope. The power consumption for the standalone cold atom flight apparatus on ISS is about 500 W [15, 16, 18]. Almost half of the power is dedicated for strong magnetic field generation for the ultra-cold atom source. An alternative design of the source would reduce the cooling power requirement by at least a factor of 10 (direct laser cooling, to be detailed on Page. 8). Thus, the total power consumption is about 300 W. Further power reduction is possible with integrated engineering efforts. Significant mass reduction is also anticipated by removing enclosure and mission-specific interfaces, potentially leading to a total instrument mass of 100 kg or less.

The spacecraft attitude control requirements for any improved MC mission are anticipated to be more stringent for better sensitivity. Our simulations show that the hybrid architecture can yield better performance just with GRACE/GRACE-FO noise models of SuperSTAR accelerometer, Star Camera Assembly (SCA), and Laser Ranging Interferometer (LRI), as illustrated in Figure 2 and Figure 4. It should also be pointed out that, using atomic test masses and measurements in a non-drag cross-track direction, there is no need for spacecraft drag-free control expected. Moreover, analyses of rotation sensitivity of the atomic gravity gradiometer define the preliminary requirements for the spacecraft stability. The rotation of the platform contributes to the AI readout and impacts the measurements in two ways. First, the differential measurement of two AIs in the gradiometer is sensitive to the centrifugal force due to the rotational motion of the spacecraft. Second, the fringe quality of each AI (fringe contrast) will be degraded by spatial fringes in the cloud, due to thermal velocity spread of the atoms, which in turn degrades the gradiometer sensitivity. Pointing inaccuracy of the gradiometer to the spacecraft cross-track direction also amplifies the degradation. It has been demonstrated that imaging readout can relax the requirements for rotation control [19-21]. Our analysis results show that there will be one spatial fringe for a 0.6 mrad misalignment toward the along-track direction, which is completely manageable by the imaging technique. On the other hand, if the gradiometer is placed radially or along-track, active rotation compensation will be needed even with the imaging technique. For gravity field inversion, it is critical to know which direction the gradient is measured, particularly for single-axis measurements as in the hybrid architecture. Fortunately, gradient is a dyad quantity so that an angular misalignment manifests itself as a second-order effect. More specifically, the cross-talk error propagation between the in-line gradients components is proportional to the second order in angle errors. The cross-talk error propagation from off-diagonal gradient elements is proportional to the first order of angular orientation error. However, the unique cross-track orientation in polar orbits reduces these errors by orders of magnitudes since the amplitude of the off-diagonal gradients that scale the angle errors are three orders of magnitude smaller than others, since these are independent of J2. This is an essential part of the advantage of the cross-track accommodation in polar orbit. The 10 μrad accuracy of SCA on GRACE-FO is already sufficient to support the pointing requirement of the hybrid architecture. Note that above estimates are based on simplified scenarios, and more rigorous end-to-end analyses are needed.

The gravity self-gradient of the spacecraft will be measurable by the atomic gravity gradiometer, even if it is placed at the center of mass. To put numbers in perspective, the self-gravity gradient of a uniform GRACE-FO spacecraft of 600 kg is 60 E in the cross-track direction

at the geometrical center. It is > 10^5 greater than the sensitivity noise floor of 200 µE. Nevertheless, the static background signal will not impact the performance of the hybrid architecture. It is because that scientifically interesting signal is time varying, and that atomic sensors measure the most significant figure by phase modulus and thus no issue on dynamic range. However, time-varying error signals can develop if the atomic clouds are not placed at the same location for each measurement with respect to the spacecraft. The precision of the atomic cloud locations will depend on the spacecraft overall mass distribution (the gradient spatial change rate) and needs analyzed and defined for a specific mass distribution. In addition, the change of mass distribution due to, e.g., thermal expansion, outgassing, fuel consumption, etc., may interfere with the interpretation of the recorded gradient data. Further study on spacecraft mass distribution stability requirement or modeling is needed.

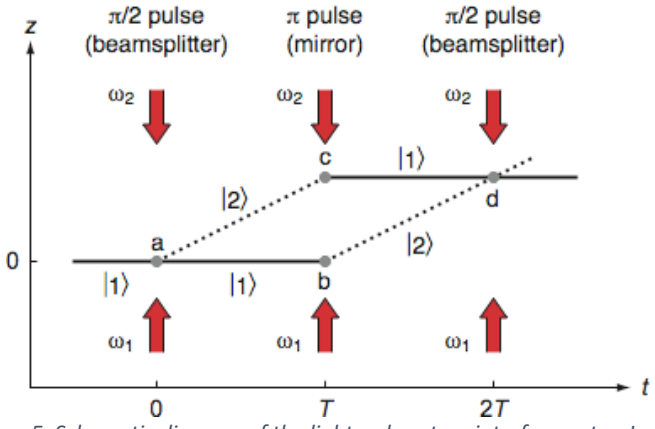

Figure 5. Schematic diagram of the light-pulse atom interferometer. In this scheme, light pulses act as beam splitters (π/2 pulses) and mirror (π pulse) for the atom waves. A phase shift results in the presence of an acceleration.

Overview of Atom Interferometer Instruments

Atom interferometers use the wave property of single atoms when the temperature is below 1µK. Laser pulses split, reflect, and recombine the wave function into two spatially different paths (Figure 5). An AI with such a three-pulse (Mach-Zehnder) configuration is sensitive to the acceleration in the direction of laser pulse propagation. The sensitivity, and the scale factor, is simply determined by the laser wavelength and the time between laser pulses [22-25], i.e., $\phi = \vec{k}_{eff} \cdot \vec{a}T^2$ where $\vec{k}_{eff}$ is the effective wavevector of the laser pulses. This simplicity makes AI accelerometers accurate over long time scales. It has been demonstrated that an AI gravimeter has measured the local gravity at Stanford, CA for four years without drift, with sensitivity better than state-of-the-art classical falling corner cube gravimeters [26]. This acceleration a has two components, $a = a_m + g$, where a_m is the motion of the AI reference point (the mirror platform) and g is the local gravitational acceleration of the falling atoms.

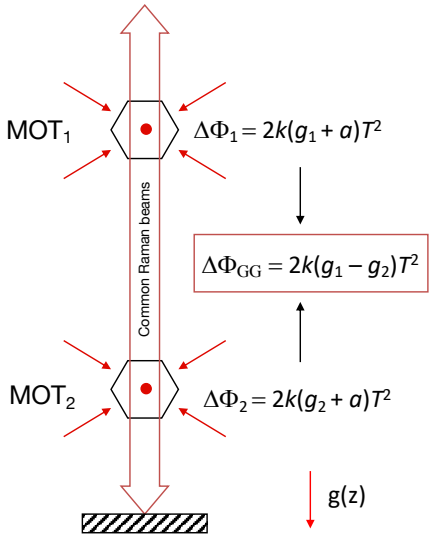

Figure 6. Schematic of an atomic gravity gradiometer.

Having two simultaneous AIs separated by h in height, the differential AI phase is then proportional to the gravity gradient γ and h (Figure 6): $\gamma = (g_1 - g_2)/h$. The impact of platform motion (a_m) is common to both and suppressed in the subtraction. The state-of-the-art performance of an atomic gravity gradiometer is about 40 $E/\sqrt{Hz}$ per 1 m separation [13, 27, 28]. These gradiometers are based on more mature cold thermal atoms of μK and the simplest interferometer scheme.

There are a number of ways to improve the gradiometer sensitivity, including a larger number of colder atoms for increased SNR, longer interrogation time T (especially in space), larger momentum transfer, and simply a longer baseline separation. For the simplest AI based on two-photon (2-$\hbar k$) beamsplitters, $\left|\vec{k}_{eff}\right| = 2\left|\vec{k}\right|$, where $\vec{k}$ is the wavevector of one of the lasers in a pulse. Development of large-momentum-transfer (LMT) technique has demonstrated that $\left|\vec{k}_{eff}\right| = 408\left|\vec{k}\right|$ is achievable [29]. On the other hand, use of LMT is not optimal for sensitivity when the AI wavepacket splitting is instrument size limited. The interrogation time T can be greatly extended from < 1 s on the ground to > 10 s under microgravity in a compact apparatus. For gravity gradient measurements, the sensitivity increases proportional to the separation h, the baseline of the gradiometer. For a given AI configuration, its sensitivity increases with the number of atoms *N,* scaling with $N^{-1/2}$, the quantum projection noise [13, 30, 31]. On the other hand, with the use of nonclassical squeezed atom states, one can beat the quantum limit, with the SNR scaling with *N* instead, in principle.

To summarize, atomic gravity gradiometer sensitivity can be increased significantly in space by using a combination of LMT, long interrogation time, long baseline, and large quantity of atoms. There are various parameter combinations for a given sensitivity requirement, and the tradeoff between their benefits, risks and complexity.

Baseline hybrid concept for the next MC mission, criteria and requirements

The hybrid architecture focuses on a design which could fit into the spacecraft configuration similar to those of the GRACE-FO mission. It can deploy single axis gradiometers to the next MC mission either as a technology demonstration or for the gravity science enhancement, or both. As depicted in Figure 1, the hybrid configuration will be a GRACE-FO spacecraft with an atomic gravity gradiometer which measures cross-track gravity gradient on each spacecraft. From our simulations as shown in Figure 4, the addition of radial or cross-track gradient data has much better impact for gravity field recovery than along-track. Moreover, the cross-track direction preferred relative to the radial or along-track directions for reasons given above, that make operation of the AI much simpler as well as geometrically compliant with the GRACE-like spacecraft.

To evaluate technology feasibility, it is beneficial to express the gradient sensitivity $\delta\gamma$ as

$$\delta\gamma = \frac{\sqrt{2}}{\left(\frac{m}{\hbar}\right) CL\Delta zT\sqrt{N}} \tag{1}$$

where m is the mass of atom (e.g., m_{Cs}=133 atomic mass unit if ^{133}Cs is used for the interferometer), $\hbar$ is the reduced Planck constant, C is the contrast of AI fringe, L is the gradiometer baseline, and Δz is the spatial extent of one AI, as depicted in Figure 7. A proper LMT is implied to reach Δz in a given interrogation time T. One can also identify that each

colored area equals ΔzT. That is, the gradient resolution is inversely proportional to the AI area, regardless how that is achieved, which could be LMT, Bloch-oscillations, or guided AI. Equation (1) represents the gradient sensitivity in terms of the critical design parameters while hiding technical detail in atomic physics. For a given size of the spacecraft , the best performance is reached by using heavy atoms, equating AI spatial extent and separation, and with a lot of atoms and a long interrogation time.

Specifically, for example, for a dimensional constraint of 1-m for the gradiometer spatial extent, i.e., $L + \Delta z = 1m$, an atomic gravity gradiometer can reach a sensitivity of 40 μE per measurement run, assuming using ^{133}Cs with C=0.5, L=0.5m, Δz=0.5m, T=15s, and N=10^8. The corresponding LMT is $\left|\vec{k}_{eff}\right| = 10\left|\vec{k}\right|$, a 10-$\hbar k$ beamsplitter AI. Here the atoms are assumed to be ultra-cold (~nK) so that all 10^8 are participating in the AI measurements at the end of the interrogation time. If the gradiometer is performed every $2T$=30s, the resulting gradient noise power spectral density (PSD) is 200 μE/$\sqrt{Hz}$. This sensitivity is at the science threshold for beyond GRACE-FO LRI, and therefore is considered as a baseline concept that can be deployed on the next GRACE-like MC mission. The sensitivity will be sufficient for data processing and analysis demonstration, and for science return beyond GRACE-FO and GOCE. If dual AIs are interleaved such that there is a 30s gradient readout every second [32], the corresponding PSD is 40 μE/$\sqrt{Hz}$. If the dimensional constraint is relaxed to 2-m, then the corresponding PSD is 10 μE/$\sqrt{Hz}$. The science measurement results with 200 μE/$\sqrt{Hz}$ and 40 μE/$\sqrt{Hz}$ instruments are plotted in Figure 8 respectively for reference.

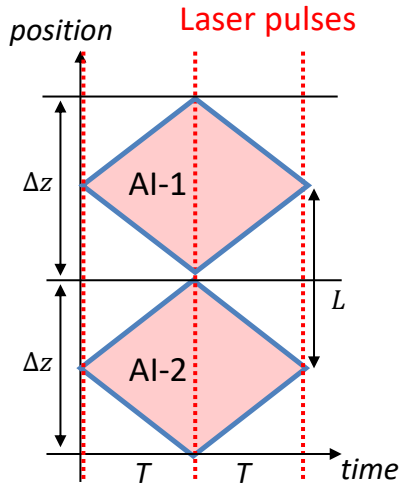

Figure 7. Space-time diagram of an atomic gravity gradiometer.

Clearly, there exists flexibility in mission and instrument design, with different concept maturity and risks as discussed below.

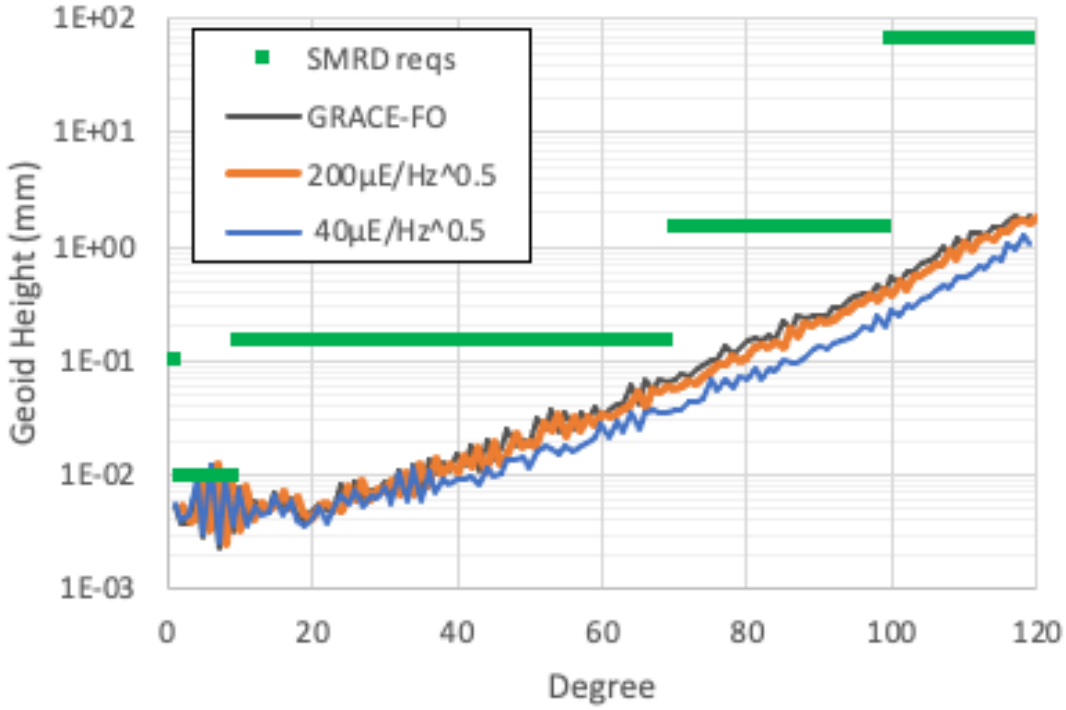

Figure 8. Simulated science measurement results at various instrument sensitivities discussed.

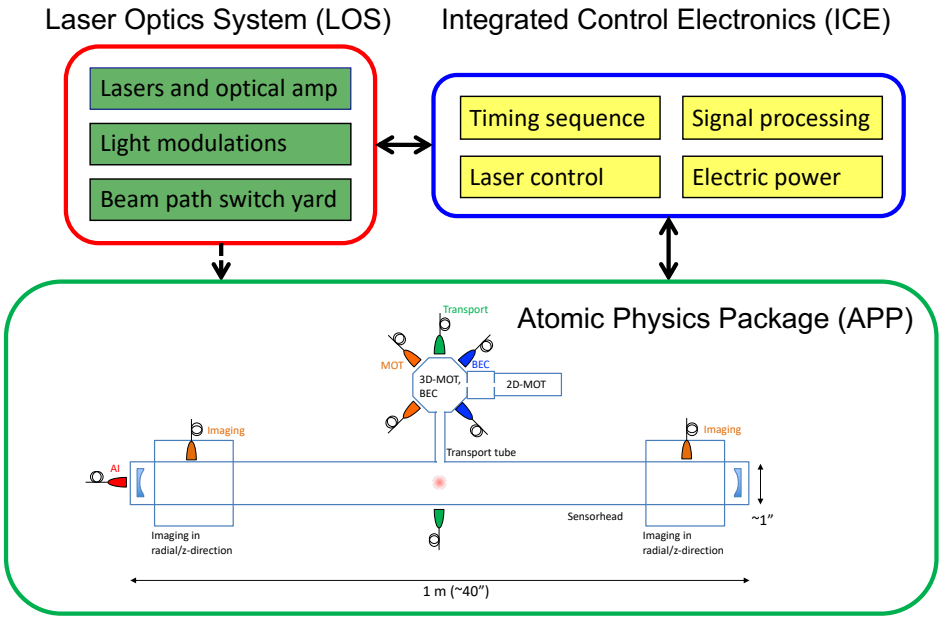

Figure 9. Schematic of the atomic gravity gradiometer for the hybrid architecture.

Instrument description and TRL

The atomic gravity gradiometer in the hybrid architecture consists of an integrated control electronics (ICE), laser and optics system (LOS), and the atomic physics package (APP), which contains the sensor-head of the gradiometer (Figure 9). Following is a brief description of the measurement operation. Cs atoms are trapped and cooled in a three-dimensional magneto-optical trap (3D-MOT), which is fed by a 2D-MOT [3]. After direct laser cooling (Possibly but not necessarily to Bose-Einstein Condensate (BEC) [33-35]), followed by delta kick cooling [15, 16, 36, 37], a cloud of 10^8 Cs atoms at sub-nK is generated at the center of the source chamber. It is then transported to the center of the sensor-head using Bloch oscillations [29, 38, 39]. The AIs will be performed inside an optical cavity of a finesse ~100 aligned in the cross-track direction. The use of the optical cavity to clean up the spatial mode was identified as crucial for retaining high contrast of AI at long interrogation times [40, 41]. After splitting the cloud into two, the dual AI accelerometers are performed using the same laser pulses inside the cavity for $2T$=30s. The LMT required for this operation will have $|\vec{k}_{eff}| = 10|\vec{k}|$, which is modest compared to state of the art. At the end of interferometer operation, the AI phase readouts are performed via absorption imaging from the side of the cavity. Figure 10 illustrates the clouds in the cavity at various steps in the AI operation procedure.

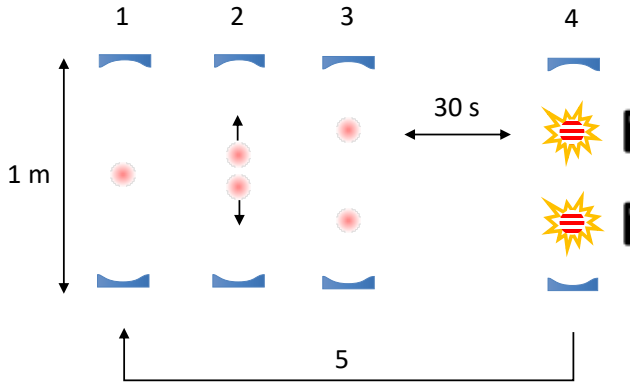

Figure 10. Depiction of AI operation in the atom interferometer cavity.

The above description conveys some of the key components and subsystems needed. Just like a precision laser interferometer requiring a high

spectral purity of sufficient power, the atom interferometer gradiometers need a high-flux ultra-cold atom source. For the future science measurement requirements of 10 μE/$\sqrt{Hz}$, 1x10^8 atoms/s at 1 nK are required. Such a source does not exist today, though a 50 nK atom source has been reported [9]. The needed atom source is one of the key technology gaps. The operation of the QGG is accomplished with a sequence of the atom cloud partition and transports. The atom transport methods have been demonstrated in research labs, but its precision over many centimeter distances needs validated [29, 38]. With many steps of laser interactions with atoms, the laser phase front inhomogeneity becomes critical. To mitigate this issue, a mode-clean cavity will be used. The cavity-based atom interferometer had also been demonstrated in research labs [40, 41], but not in precision measurement configurations yet. In addition, several potential risks associated with long interrogation times (up to 20 sec in space) need to be retired. On the hardware side, the key subsystems of vacuum enclosure and laser system must be space qualified. A detailed assessment of component TRLs and new technology developments are summarized Figure 11. It starts at a baseline configuration of 600 μE/$\sqrt{Hz}$ with the specific approaches that have been demonstrated in research labs separately, and progresses through a set of the new technology developments towards achieving the full QGG potential with 10 μE/$\sqrt{Hz}$.

The baseline instrument maturation can be realized in the next five years as summarized in the Table of maturation plan in Figure 12. With additional parallel efforts of the new technology developments, they can be infused into the baseline approach to enhance the instrument performances. If one of the new technologies gets infused in time, the QGG performance can be significantly enhanced. The infusions can be more of an add-on in the architecture in nature rather than disruptive new designs.

However, one of the main challenges in instrument maturation and validation is the fact that the actual performance can only be achieved and validated under a proper microgravity environment of long duration. One can test and validate most of the operations of the instrument on the ground, but it is risky to extrapolate the space measurement precision from the ground measurements by a factor of over 1,000. As such, microgravity validation experiments must be performed to adequately validate the measurement concept before developing flight the mission instrument, or a pathfinder demo mission before a full science mission implementation. ISS is perhaps the best platform for such validation experiments, short of a satellite mission itself. Sounding rockets and ground drop towers, especially the Einstein Elevator at Hannover Institute of Technology in Germany [42, 43], can provide most of the microgravity operation tests, but likely not the precision needed. Zero-G flights do not have a good enough microgravity environment nor attitude controls to be useful. Accordingly, a technology maturation roadmap as outlined in Figure 11, has been generated through an JPL internal study in collaboration with CSR of UT Austin. It aims at maturing components while developing a test instrument to be validated in a microgravity platform to advance the instrument and measurement concept to TRL6.

There are a number of other institutions with the relevant research, development, and product capabilities to possibly support an overall technology maturation effort, including GSFC (QGG IIP, single gradiometer study), UC Berkeley (LMT, atom transport, cavity), Stanford U (AI, gradiometer, 10 m fountain), AOsense (IIP gradiometer, gravimeter, and laser components),

ColdQuanta (BEC machine, cold atom components), Vescent (lasers), ADVR (lasers, nonlinear crystals), Photodigm (laser chips), and many other small companies. Similar development efforts exit in Europe, in particular within DLR and CNES. International collaborations are possible and interests are shared.

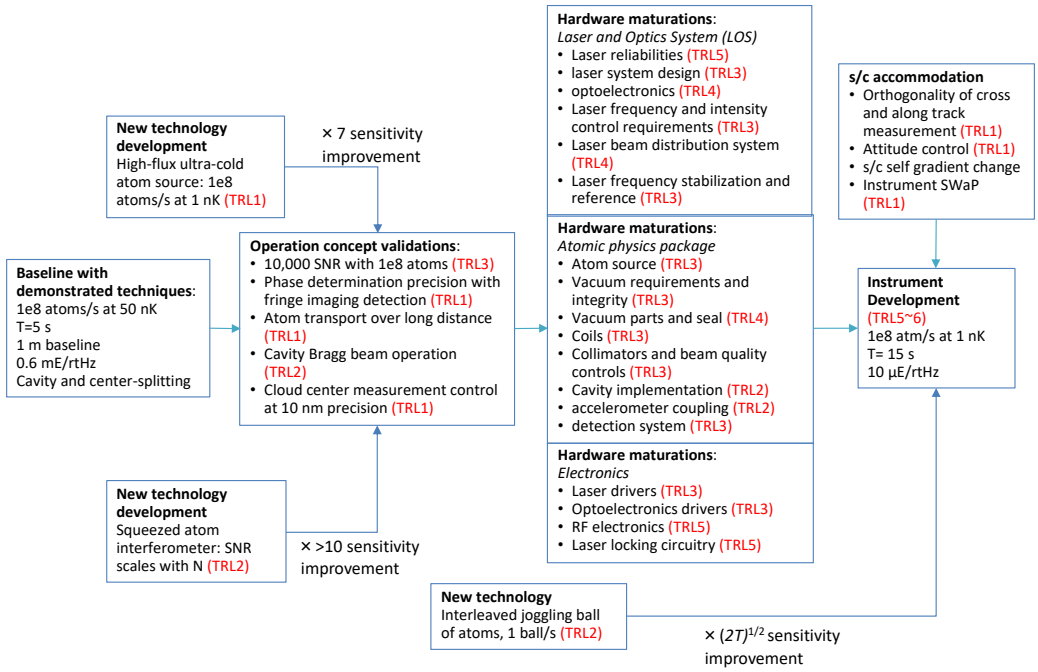

Figure 11. State of the art and instrument maturation plan.

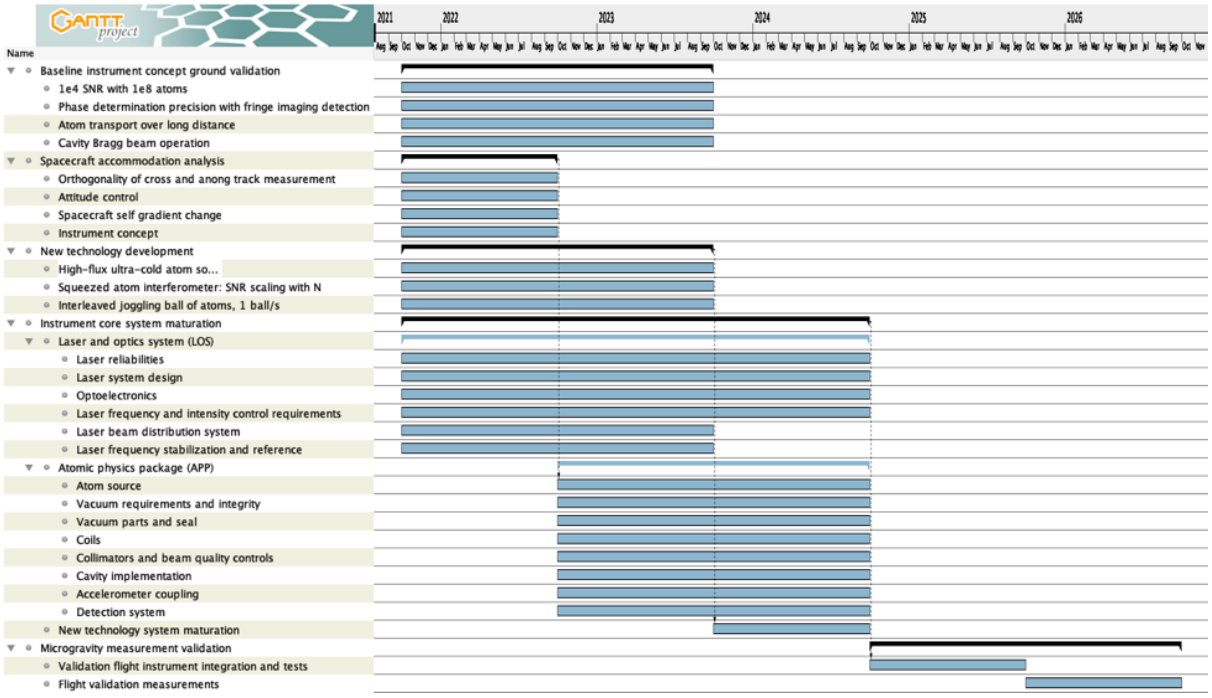

Figure 12. Instrument maturation schedule.

References

[1] N. Yu, J. M. Kohel, L. Romans, and L. Maleki, "Quantum gravity gradiometer sensor for earth science applications," presented at the NASA Earth Science Technology Conference, 2002. [Online]. Available: https://citeseerx.ist.psu.edu/viewdoc/download?doi=10.1.1.484.4053&rep=rep1&type=pdf.

[2] J. Johannessen, "Gravity Field and Steady-Stat Ocean Circulation Mission. Reports for Mission Selection," *ESA SP,* vol. 1233, no. 1, 1999.

[3] N. Yu, J. M. Kohel, J. R. Kellogg, and L. Maleki, "Development of an atom-interferometer gravity gradiometer for gravity measurement from space," *Appl Phys B-Lasers O,* vol. 84, no. 4, pp. 647, Sep 2006. DOI: http://doi.org/10.1007/s00340-006-2376-x

[4] S. B. Luthcke, D. D. Rowlands, B. Saif, and A. Black, "Earth time variable gravity from a spaceborne cold atom gravity gradiometer," presented at the AGU Fall Meeting Abstracts, December 01, 2013, 2013. [Online]. Available: https://ui.adsabs.harvard.edu/abs/2013AGUFM.G11A0905L.

[5] S. B. Luthcke, B. Saif, A. Black, and D. D. Rowlands, "Earth Time Variable Gravity from a Spaceborne Cold Atom Gravity Gradiometer," presented at the AGU Fall Meeting Abstracts, December 01, 2014, 2014. [Online]. Available: https://ui.adsabs.harvard.edu/abs/2014AGUFM.G23C..07L.

[6] A. Sugarbaker *et al.*, "Cold Atom Gravity Gradiometer for Geodesy," presented at the APS Division of Atomic, Molecular and Optical Physics Meeting Abstracts, May 01, 2015, 2015. [Online]. Available: https://ui.adsabs.harvard.edu/abs/2015APS..DMP.K1066S.

[7] S. B. Luthcke, B. Saif, A. Sugarbaker, D. D. Rowlands, and B. Loomis, "Development and Performance of an Atomic Interferometer Gravity Gradiometer for Earth Science," presented at the AGU Fall Meeting Abstracts, December 01, 2016, 2016. [Online]. Available: https://ui.adsabs.harvard.edu/abs/2016AGUFM.G53A..06L.

[8] A. Rakholia *et al.*, "Development of an Atom Interferometer Gravity Gradiometer for Earth Sciences," presented at the APS Division of Atomic, Molecular and Optical Physics Meeting Abstracts, April 01, 2017, 2017. [Online]. Available: https://ui.adsabs.harvard.edu/abs/2017APS..DMP.K1010R https://ntrs.nasa.gov/archive/nasa/casi.ntrs.nasa.gov/20170005272.pdf.

[9] B. Saif, S. Luthcke, L. Callahan, A. Sugarbaker, and A. Rakholia, "AI Gravity Gradiometer for Earth Science," presented at the ESA'S QUANTUM TECHNOLOGY – IMPLEMENTATIONS FOR SPACE WORKSHOP, Noordvijk, Netherlands, 2017.

[10] "GRACE." https://directory.eoportal.org/web/eoportal/satellite-missions/g/grace.

[11] "GRACE-FO." https://directory.eoportal.org/web/eoportal/satellite-missions/g/grace-fo.

[12] H. Save, S. Bettadpur, and B. D. Tapley, "High-resolution CSR GRACE RL05 mascons," *J Geophys Res-Sol Ea,* vol. 121, no. 10, pp. 7547, Oct 2016. DOI: http://doi.org/10.1002/2016jb013007

[13] S. W. Chiow, J. Williams, and N. Yu, "Noise reduction in differential phase extraction of dual atom interferometers using an active servo loop," *Phys Rev A,* vol. 93, no. 1, Jan 6 2016. DOI: http://doi.org/10.1103/PhysRevA.93.013602

[14] "Muquans.com." https://www.muquans.com/.

[15] E. R. Elliott, M. C. Krutzik, J. R. Williams, R. J. Thompson, and D. C. Aveline, "NASA's Cold Atom Lab (CAL): system development and ground test status," *NPJ Microgravity,* vol. 4, no. 1, p. 16, 2018. DOI: http://doi.org/10.1038/s41526-018-0049-9

[16] D. C. Aveline *et al.*, "Observation of Bose–Einstein condensates in an Earth-orbiting research lab," *Nature,* vol. 582, no. 7811, pp. 193, Jun 2020. DOI: http://doi.org/10.1038/s41586-020-2346-1

[17] M. D. Rosen, "Analysis of hybrid satellite-to-satellite tracking and quantum gravity gradiometry architecture for time-variable gravity sensing missions," 2021. [Online]. Available: https://hdl.handle.net/2152/87597 https://repositories.lib.utexas.edu/bitstream/handle/2152/87597/ROSEN-THESIS-2021.pdf?sequence=1

[18] K. Frye *et al.*, "The Bose-Einstein Condensate and Cold Atom Laboratory," *Epj Quantum Technol,* vol. 8, no. 1, Jan 2021. DOI: http://doi.org/10.1140/epjqt/s40507-020-00090-8

[19] S. M. Dickerson, J. M. Hogan, A. Sugarbaker, D. M. Johnson, and M. A. Kasevich, "Multiaxis inertial sensing with long-time point source atom interferometry," *Phys Rev Lett,* vol. 111, no. 8, p. 083001, Aug 23 2013. DOI: http://doi.org/10.1103/PhysRevLett.111.083001

[20] A. Sugarbaker, S. M. Dickerson, J. M. Hogan, D. M. Johnson, and M. A. Kasevich, "Enhanced atom interferometer readout through the application of phase shear," *Phys Rev Lett,* vol. 111, no. 11, p. 113002, Sep 13 2013. DOI: http://doi.org/10.1103/PhysRevLett.111.113002

[21] Y. J. Chen, A. Hansen, M. Shuker, R. Boudot, J. Kitching, and E. A. Donley, "Robust inertial sensing with point-source atom interferometry for interferograms spanning a partial

period," *Opt Express,* vol. 28, no. 23, pp. 34516, Nov 9 2020. DOI: http://doi.org/10.1364/OE.399988

[22] C. J. Borde, "Atomic Interferometry with Internal State Labeling," *Phys Lett A,* vol. 140, no. 1-2, pp. 10, Sep 4 1989. DOI: http://doi.org/10.1016/0375-9601(89)90537-9

[23] M. Kasevich and S. Chu, "Atomic Interferometry Using Stimulated Raman Transitions," *Phys Rev Lett,* vol. 67, no. 2, pp. 181, Jul 8 1991. [Online]. Available: <Go to ISI>://WOS:A1991FV18200006

[24] G. Stern *et al.*, "Light-pulse atom interferometry in microgravity," *Eur Phys J D,* vol. 53, no. 3, pp. 353, Jun 2009. DOI: http://doi.org/10.1140/epjd/e2009-00150-5

[25] G. Tino *et al.*, "Atom interferometers and optical atomic clocks: New quantum sensors for fundamental physics experiments in space," *Nuclear Physics B (Proceedings Supplements),* vol. 166, pp. 159, 2007.

[26] K. Y. Chung, S. W. Chiow, S. Herrmann, S. Chu, and H. Müller, "Atom interferometry tests of local Lorentz invariance in gravity and electrodynamics," *Phys Rev D,* vol. 80, no. 1, Jul 2009. DOI: http://doi.org/10.1103/PhysRevD.80.016002

[27] J. M. McGuirk, G. T. Foster, J. B. Fixler, M. J. Snadden, and M. A. Kasevich, "Sensitive absolute-gravity gradiometry using atom interferometry," *Phys Rev A,* vol. 65, no. 3, Mar 2002. DOI: http://doi.org/10.1103/PhysRevA.65.033608

[28] G. W. Biedermann, X. Wu, L. Deslauriers, S. Roy, C. Mahadeswaraswamy, and M. A. Kasevich, "Testing gravity with cold-atom interferometers," *Phys Rev A,* vol. 91, no. 3, p. 033629, March 01, 2015 2015. DOI: http://doi.org/10.1103/PhysRevA.91.033629

[29] M. Gebbe *et al.*, "Twin-lattice atom interferometry," p. arXiv:1907.08416 https://ui.adsabs.harvard.edu/abs/2019arXiv190708416G

[30] W. M. Itano *et al.*, "Quantum Projection Noise - Population Fluctuations in 2-Level Systems," *Phys Rev A,* vol. 47, no. 5, pp. 3554, May 1993. DOI: http://doi.org/10.1103/PhysRevA.47.3554

[31] F. Sorrentino *et al.*, "Sensitivity limits of a Raman atom interferometer as a gravity gradiometer," *Phys Rev A,* vol. 89, no. 2, Feb 10 2014. DOI: http://doi.org/10.1103/PhysRevA.89.023607

[32] D. Savoie, M. Altorio, B. Fang, L. Sidorenkov, R. Geiger, and A. Landragin, "Interleaved atom interferometry for high-sensitivity inertial measurements," *Science advances,* vol. 4, no. 12, p. eaau7948, Dec 2018. DOI: http://doi.org/10.1126/sciadv.aau7948

[33] P. Solano, Y. Duan, Y.-T. Chen, A. Rudelis, C. Chin, and V. Vuletić, "Strongly Correlated Quantum Gas Prepared by Direct Laser Cooling," *Phys Rev Lett,* vol. 123, no. 17, p. 173401, 10/24/ 2019. DOI: http://doi.org/10.1103/PhysRevLett.123.173401

[34] J. Z. Hu, A. Urvoy, Z. Vendeiro, V. Crepel, W. Chen, and V. Vuletic, "Creation of a Bose-condensed gas of Rb-87 by laser cooling," *Science,* vol. 358, no. 6366, pp. 1078, Nov 24 2017. DOI: http://doi.org/10.1126/science.aan5614

[35] A. Urvoy, Z. Vendeiro, J. Ramette, A. Adiyatullin, and V. Vuletic, "Direct Laser Cooling to Bose-Einstein Condensation in a Dipole Trap," *Phys Rev Lett,* vol. 122, no. 20, p. 203202, May 24 2019. DOI: http://doi.org/10.1103/PhysRevLett.122.203202

[36] H. Müntinga *et al.*, "Interferometry with Bose-Einstein Condensates in Microgravity," *Phys Rev Lett,* vol. 110, no. 9, p. 093602, Mar 1 2013. DOI: http://doi.org/10.1103/PhysRevLett.110.093602

[37] M. Meister, A. Roura, E. M. Rasel, and W. P. Schleich, "The space atom laser: an isotropic source for ultra-cold atoms in microgravity," *New J Phys,* vol. 21, Jan 31 2019. DOI: http://doi.org/10.1088/1367-2630/aaf7b5

[38] Z. Pagel, W. Zhong, R. H. Parker, C. T. Olund, N. Y. Yao, and H. Müller, "Symmetric Bloch oscillations of matter waves," *Phys Rev A,* vol. 102, no. 5, p. 053312, 11/13/ 2020. DOI: http://doi.org/10.1103/PhysRevA.102.053312

[39] J. Williams, S.-w. Chiow, N. Yu, and H. Müller, "Quantum test of the equivalence principle and space-time aboard the International Space Station," *New J Phys,* vol. 18, no. 2, p. 025018, 2016/02/17 2016. DOI: http://doi.org/10.1088/1367-2630/18/2/025018

[40] M. Dovale-Álvarez, D. D. Brown, A. W. Jones, C. M. Mow-Lowry, H. Miao, and A. Freise, "Fundamental limitations of cavity-assisted atom interferometry," *Phys Rev A,* vol. 96, no. 5, p. 053820, 11/08/ 2017. DOI: http://doi.org/10.1103/PhysRevA.96.053820

[41] V. Xu, M. Jaffe, C. D. Panda, S. L. Kristensen, L. W. Clark, and H. Müller, "Probing gravity by holding atoms for 20 seconds," *Science,* vol. 366, no. 6466, pp. 745, Nov 8 2019. DOI: http://doi.org/10.1126/science.aay6428

[42] "EE@HITec." https://www.hitec.uni-hannover.de/en/large-scale-equipment/einstein-elevator/.

[43] C. Lotz, T. Froböse, A. Wanner, L. Overmeyer, and W. Ertmer, "Einstein-Elevator: A New Facility for Research from µg to 5 g," *Gravitational and Space Research,* vol. 5, no. 2, 2017.